

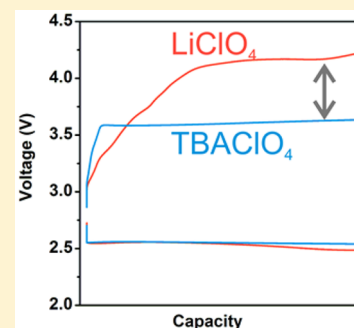
Influence of Ammonium Salts on Discharge and Charge of Li–O₂ Batteries

Chibueze V. Amanchukwu,^{†,‡} Hao-Hsun Chang,[§] and Paula T. Hammond^{*,†,‡,§}

[†]Department of Chemical Engineering, [‡]The David H. Koch Institute for Integrative Cancer Research, and [§]Electrochemical Energy Laboratory, Research Laboratory of Electronics, Massachusetts Institute of Technology, Cambridge, Massachusetts 02139, United States

Supporting Information

ABSTRACT: Li–air (O₂) batteries are promising because of their high theoretical energy density. However, these batteries are plagued with numerous challenges, one of which involves modulating the battery discharge process between a solution or surface-driven formation of the desired lithium peroxide (Li₂O₂) discharge product, and the oxidation of Li₂O₂ below 4 V (vs Li/Li⁺). In this work, we show that tetrabutylammonium (TBA) salts dissolved in ether or dimethyl sulfoxide (with no lithium salt present) can be used as a Li–O₂ electrolyte with a lithium metal anode to support Li₂O₂ formation, lead to >500 mV reduction in charging overpotentials at low current rates as compared to that with lithium salt, and support the oxidation of Li₂O₂ during charge. Furthermore, on the basis of results from several spectroscopic techniques, we propose a mechanism that involves electrochemical-induced transformation of TBA to tributylamine at ~3.55 V, and the formation of a tributylamine oxide intermediate in the presence of O₂ or Li₂O₂ that is responsible for Li₂O₂ oxidation during charging. This mechanism can also be translated to other ionic liquid-based Li–O₂ batteries where significantly low charging potentials are observed. This work showcases an additive that can be used for Li–O₂ batteries to allow for finer control of the discharge process, and the ability of amine oxides to oxidize Li₂O₂.



INTRODUCTION

Energy storage media such as batteries and fuel cells are vital in the drive to reduce fossil fuel use in transportation and electricity generation.^{1–3} Newer energy-dense battery chemistries are being explored,¹ and, of these, Li–air (O₂) batteries with a theoretical gravimetric energy density of 3500 Wh/kg_{Li₂O₂} as compared to 200 Wh/kg for Li-ion have shown great promise.^{1,2,4} Li–O₂ chemistry is governed by oxygen reduction and evolution during discharge and charge, respectively.^{5,6} During discharge, oxygen is reduced at the cathode to produce superoxide (Scheme 1).^{5,7} Once formed, superoxide is a soft base that according to hard soft acid base (HSAB) theory prefers stabilization by a bulky cation (soft acid).^{8,9} However, the presence of Li⁺ in the electrolyte leads to LiO₂ (lithium superoxide),¹⁰ a highly reactive and unstable intermediate.¹¹ Disproportionation of LiO₂ or a further electron transfer step leads to Li₂O₂ (lithium peroxide).^{5,7} Charging of Li–O₂ cells involves decomposition of Li₂O₂ to release Li⁺ and O₂.⁶ Because Li₂O₂ is an insulator with high bandgap and low electronic conductivity,¹² high overpotentials are observed during charging. Side reactions between LiO₂ (or Li₂O₂) with the electrolyte solvent,¹³ salt,¹⁴ and electrodes¹⁵ lead to unwanted side products such as LiOH,¹³ Li₂CO₃,¹⁶ and LiF¹¹ among others that also require much higher charging overpotentials to oxidize, leading to low energy efficiencies, poor capacity retention with cycling, and limited cycle life.^{5,17}

Several strategies have been pursued to mediate the discharge and charge processes to improve discharge capacity and

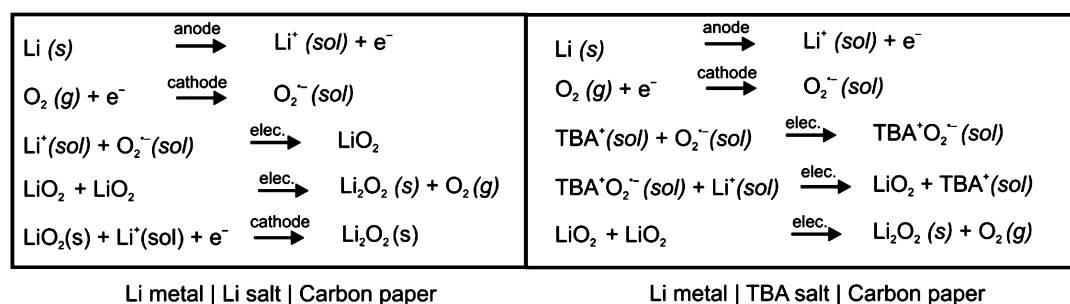
capacity retention with cycling. For charging, metal/metal oxide catalysts¹⁸ and redox mediators such as LiI¹⁹ and tetrathiafulvalene (TTF)²⁰ have been added to the electrode or electrolyte to reduce the charging voltages below 4 V. Reducing charging hysteresis is vital to improve energy efficiencies, but also because the most stable family of solvents for Li–O₂ batteries are glymes, which are electrochemically unstable above 4 V.²¹ For discharge, a solution-mediated formation of Li₂O₂ discharge product, where toroids are formed, leads to better utilization of the cathode and higher discharge capacities,^{22,23} whereas a surface-driven formation leads to film growth on the electrode. Because Li₂O₂ is an insulator, it blocks further O₂ reduction and lowers the discharge capacity. However, compared to toroids, Li₂O₂ films are easier to remove during charge because of their proximity to the electrode.^{24,25} The Li₂O₂ growth mechanism is typically rate-dependent with low current rates favoring a solution-based mechanism, and high current rates favoring surface formation, but other parameters such as solvent type,²⁴ salt anion,²³ and additives (H₂O, etc.)²² have been explored to modulate Li₂O₂ growth.

The ability of a solvent to support the solution-mediated formation of Li₂O₂ is correlated with its susceptibility to nucleophilic attack.^{22,26} For example, as one increases the solvent donor number (ability of solvent to donate electron

Received: May 31, 2017

Revised: July 14, 2017

Published: August 1, 2017

Scheme 1. Li–O₂ Cell Discharge Mechanisms^a

^aProposed discharge reaction mechanism when lithium salt is dissolved in the electrolyte as compared to when TBAClO₄ salt is dissolved in the electrolyte. The anion (e.g., ClO₄[−]) is omitted in the scheme for clarity. Anode and cathode are lithium metal and carbon paper, respectively. TBA = tetrabutylammonium; “elec.” = electrolyte; “s” = solid; “g” = gas; “sol” = solution.

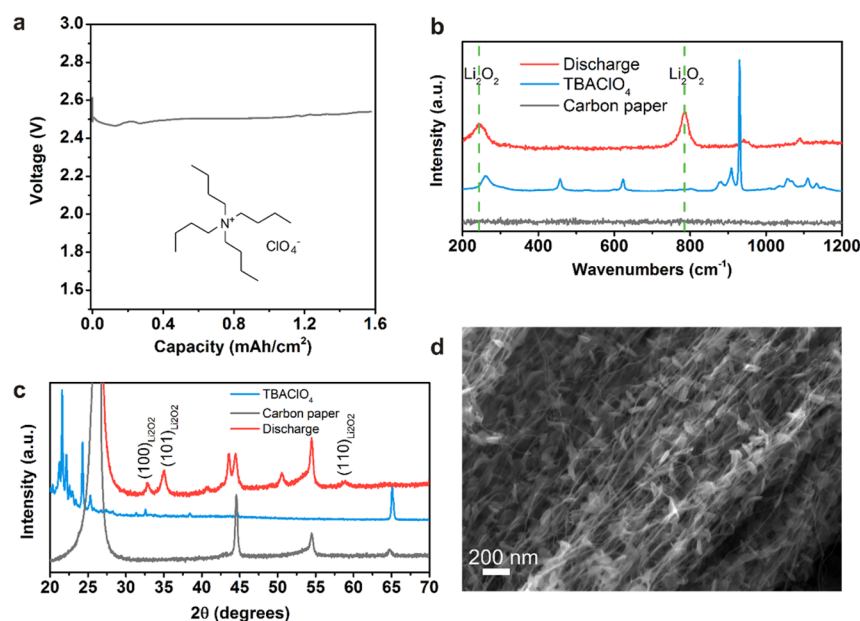


Figure 1. Discharge behavior using a TBAClO₄-only electrolyte. (a) Discharge curve, (b) Raman, (c) XRD, and (d) SEM after discharge at 15.7 μA/cm² (geometric surface area) in oxygen using 0.1 M TBAClO₄ in DME as the electrolyte. Inset in (a) is the chemical structure of tetrabutylammonium perchlorate. Voltage (vs Li/Li⁺). Li–O₂ cell setup for (a)–(c): Li metal|0.1 M TBAClO₄ in DME|carbon paper. Li–O₂ cell setup for (d): Li metal|0.1 M TBAClO₄ in DME|carbon nanotube.

density to an acceptor or Lewis acid)²⁷ from acetonitrile, DME, to DMSO, the vulnerability of the solvent to nucleophilic attack increases.²⁶ Therefore, it is important to modulate the solution-based mechanism by varying additives in one solvent (instead of changing solvents), preferably in glyme solvents.²³ Burke et al.²³ varied anion (NO₃[−]) concentration in DME to improve Li⁺ solvation and induce solution-mediated Li₂O₂ formation, but solubility of LiNO₃ in ethers is limited, and nitrate will be irreversibly consumed in creating a solid electrolyte interface (SEI) layer on the lithium metal anode.^{28,29} Other researchers have shown that added H₂O in the electrolyte directs toroidal and crystalline Li₂O₂ growth through a solution-driven process,^{22,30} but LiOH formation or other side reactions with lithium metal limits the utility of added H₂O. However, cation type has not been evaluated because it has been widely assumed (as expected) that a lithium salt was required for Li–O₂ discharge. The larger a cation is, the “softer” it is, and the more stable is the cation–superoxide complex, where cations such as pyrrolidinium³¹ and ammonium³² can coordinate and stabilize superoxide at longer time scales than lithium.³³

Therefore, investigating the influence of the presence of bulkier cations as an additional knob for controlling Li–O₂ battery chemistry is vital.

The oxygen reduction and evolution process in nonaqueous systems has been heavily studied using ammonium-based salts as supporting electrolytes.^{7,9,34} Tetrabutylammonium (TBA) salts can form stable TBA–superoxide complexes³² during oxygen reduction, and these complexes can be reversibly oxidized without external catalysts.⁷ Although TBA-influenced oxygen reduction and evolution has been investigated using cyclic voltammetry,^{7,9} the influence of TBA on the electrochemical performance of actual Li–O₂ batteries has not been explored.

In this work, we study the ability of a non-lithium salt to support a solution-driven formation of Li₂O₂ in Li–O₂ batteries. We exploit the ability of TBA to sequester superoxide, and fabricate Li–O₂ cells using TBAClO₄ (Figure 1a, inset) as the only dissolved salt. Similar to the use of viologen³⁵ and 2,5-di-*tert*-butyl-1,4-benzoquinone,²⁵ TBA supports a solution-driven formation of Li₂O₂, a discharge product formed despite

the lack of lithium salt present (Scheme 1). The influence of current rate, TBA concentration, and solvent type on the ability of TBA to support Li–O₂ discharge and charge was also explored. Interestingly, we observe that the presence of TBA in the electrolyte leads to much lower charging overpotentials (500 mV difference) than when a lithium salt is used. Using Li₂O₂-preloaded cells, we further show that the presence of TBA at potentials below 4 V is capable of oxidizing Li₂O₂, unlike typically used lithium salts like LiClO₄. Given the results from several spectroscopic tools, we propose a mechanism that involves the electrochemical-induced transformation of TBA to tributylamine, and the formation of a tributylamine oxide intermediate in the presence of O₂ or Li₂O₂ that can oxidize Li₂O₂ below 4 V. This work shows the evaluation of a Li–O₂ cell with no added lithium salt present in the electrolyte, the influence of ammonium salts on the discharge/charge behavior of Li–O₂ cells, and the use of amine oxides to oxidize Li₂O₂. Knowledge gained should provide insight into a new class of potential salts for metal-air use, and new pathways to oxidize Li₂O₂ during charge.

METHODS

Materials. Tetrabutylammonium perchlorate (>99%), lithium perchlorate, diethylene glycol dimethyl ether (diglyme), 1,2-dimethoxyethane (anhydrous), acetonitrile, dimethyl sulfoxide (anhydrous), lithium peroxide (90%), tributylamine, 1-decene, trimethylamine oxide, and quinine were obtained from Sigma-Aldrich. Carbon paper (TGP-H-60, not PTFE treated) and lithium metal (0.75 mm thick, 99.9%) were obtained from Alfa Aesar. Nafion was obtained as a 7.2 wt % lithiated Nafion in isopropanol solution from Ion Power Inc. Celgard C480 was obtained from Celgard. DMSO-*d*₆ (with or without 0.03 v/v % tetramethylsilane) was obtained from Cambridge Isotope. Whatman GF/A separator was obtained from GE Life Sciences. Vulcan carbon (Vulcan XC72, 100 m²/g) was obtained from Premetek Inc.

The solvents (DME, diglyme, and DMSO) were stored with molecular sieves (4 Å) in an argon glovebox (MBRAUN, H₂O < 0.1 ppm, O₂ < 0.1 ppm), and the electrolyte (salt dissolved in solvent) was made in the glovebox just before fabricating the Li–O₂ cell to limit exposure to water. Measured water content of the electrolytes was less than 30 ppm (using Karl Fischer).

Electrode Fabrication. The carbon paper electrodes were cut into 12.7 mm diameter disks and vacuum-dried at 75 °C overnight. The Li₂O₂ preloaded electrodes were fabricated in a 1:1:1 mass ratio of Vulcan carbon:Li₂O₂:lithiated Nafion, and deposited on aluminum foil in the same manner as described in ref 18. The electrodes were transferred to the glovebox without ambient exposure. The carbon nanotube (CNT) carpets were fabricated as previously reported by Gallant et al.,³⁶ and vacuum-dried at 75 °C overnight before being transferred and stored in an argon glovebox (MBRAUN, H₂O < 0.1 ppm, O₂ < 0.1 ppm) without ambient exposure.

Electrochemical Testing. Lithium metal (15 mm diameter) was used as the anode and carbon paper (12.7 mm diameter) as the cathode. 120 μL of 0.1 M TBAClO₄ or 0.1 M LiClO₄ in DME solution and 0.1 M TBAClO₄ or 0.1 M LiClO₄ in DMSO was used. For the 2:1 molar ratio TBAClO₄/LiClO₄ electrolyte mixture, the 0.1 M TBAClO₄ in DME and the 0.1 M LiClO₄ in DME solutions were not premixed before making the Li–O₂ cell. 40 μL of the 0.1 M LiClO₄ in DME solution was first added to the Li–O₂ cell before 80 μL of 0.1 M TBAClO₄ in DME was added. Two Celgard C480 separators were used

for all DME Li–O₂ cells, while one Whatman separator was used for the DMSO Li–O₂ cells. Li–O₂ cells were fabricated in an argon glovebox (MBRAUN, H₂O < 0.1 ppm, O₂ < 0.1 ppm). The cells were then transferred to another Argon glovebox (MBRAUN, H₂O < 0.1 ppm, O₂ < 1%) without air exposure and pressurized with either argon or oxygen gas. The cells were allowed to rest at open circuit voltage (OCV) for at least 4 h before electrochemical measurements were performed. A VMP3 (BioLogic Inc.) was used for all electrochemical tests.

Cyclic voltammetry (two-electrode setup) was performed using the same Li–O₂ cell setup as above. Lithium metal (15 mm diameter) served as both reference and counter electrodes. Carbon paper (12.7 mm diameter) served as the working electrode. The cell was fabricated in an argon glovebox (MBRAUN, H₂O < 0.1 ppm, O₂ < 0.1 ppm) and was pressurized with either argon or oxygen (without air exposure) in a manner similar to the paragraph above. The cell was allowed to rest at OCV for at least 4 h before electrochemical measurements were performed. A sweep rate of 0.1 mV/s was used from 1.5 to 4.5 V.

Potentiostatic Li₂O₂ Preloaded Cells. The Li₂O₂ preloaded cells were fabricated in a manner similar to that of the Li–O₂ cells. A lithium metal anode (15 mm diameter) was used as the negative electrode, and 90 μL of either LiClO₄ or TBAClO₄ in diglyme or 120 μL of TBAClO₄ in DMSO was used as the electrolyte. The Vulcan carbon/Li₂O₂/Nafion (1:1:1 mass ratio) on aluminum foil was used as the positive electrode. For the cell without Li₂O₂ present, a Vulcan carbon/Nafion (1:1 mass ratio) on Celgard electrode was used. The cells were allowed to rest for at least 5 h at OCV, before the potentiostatic tests were performed. For cells held at oxidizing voltages (e.g., 3.7 and 3.9 V), the cell was held at 2.9 V for 30 min before continuing at the oxidizing voltage for the stated time (100 or 200 h).

Chemical Mixtures with Li₂O₂ or KO₂. All experiments were performed in an inert glovebox atmosphere (argon or nitrogen). Vials were stirred for 3 days.

(a) Tributylamine: In a 5 mL vial, 15 mg of Li₂O₂ and 0.3 mL of tributylamine.

(b) 1-Decene: In a 5 mL vial, 15 mg of Li₂O₂ and 0.3 mL of 1-decene.

(c) Trimethylamineoxide: 1:1 molar ratio of TMAO:Li₂O₂ in acetonitrile.

(d) TBAClO₄: In a 20 mL vial, a 10:10:1 molar ratio of KO₂:Li₂O₂:TBAClO₄ was added to acetonitrile and stirred for 3 days.

The TBAClO₄/KO₂/Li₂O₂, tributylamine/Li₂O₂, and 1-decene/Li₂O₂ mixtures were allowed to settle, and the remaining Li₂O₂ was allowed to sediment. About 20 μL of each supernatant was added to DMSO-*d*₆ for ¹H NMR analysis. For the TMAO/Li₂O₂ mixture, acetonitrile was removed from the vial, and DMSO-*d*₆ was then added for ¹H NMR.

Characterization Techniques. X-ray Diffraction (XRD). XRD data were obtained using a Rigaku Smartlab (Rigaku, Salem, NH) in the parallel beam configuration with a Cu Kα radiation source. Electrochemically tested samples were opened in an argon glovebox, and sealed in an airtight XRD sample holder (Anton Paar, Austria) for XRD measurement. The reference code (01-074-0115) was used for all of the Li₂O₂ references in the XRD spectra.

Raman Spectroscopy. Raman data were obtained using a LabRAM Hr800 microscope (HORIBA) with an external 633 nm laser, with a 50× long working distance lens. A silicon wafer

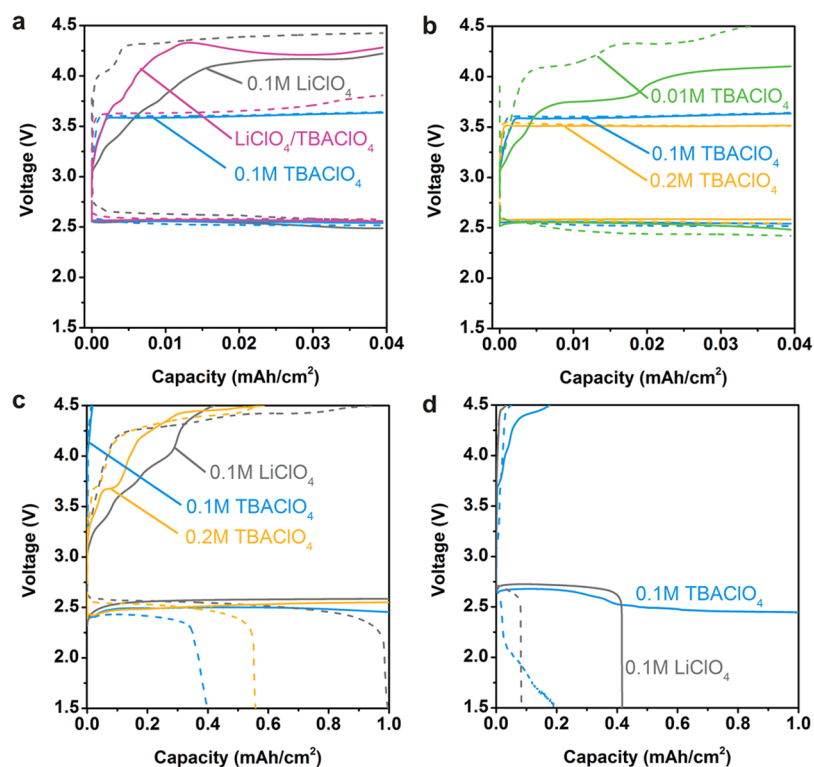


Figure 2. Effect of TBA and Li salt on Li–O₂ cycling in DME and DMSO at different current rates. Cycling of a Li–O₂ cell in oxygen in DME at 3.95 $\mu\text{A}/\text{cm}^2$ to a 0.04 mAh/cm^2 cutoff with (a) different electrolyte salt content and (b) different TBA concentration. The LiClO₄/TBAClO₄ electrolyte is a 2:1 molar ratio of TBAClO₄:LiClO₄ in DME. Cycling in oxygen at 100 $\mu\text{A}/\text{cm}^2$ to a 1 mAh/cm^2 cutoff with (c) DME and (d) DMSO electrolytes. Concentrations are as shown in the figures in the respective solvents (a–c, DME; d, DMSO). (Bold lines) first cycle; (Dashed lines) fifth cycle. Voltages are vs Li/Li⁺. Current rates and capacities are based on the geometric surface area of the carbon paper electrode. Li–O₂ cell setup: Li metal(TBAClO₄ or LiClO₄) in DMSO or DME|carbon paper.

was used for calibration. A sealed custom-designed airtight Raman cell was used for the electrochemically tested samples.

Scanning Electron Microscope (SEM). SEM images were captured using a ZEISS Merlion (Carl Zeiss Microscopy GmbH, Germany) with an in-lens detector at 10 kV and 127 pA. Samples were sealed in aluminum foil bags in an argon-filled glovebox and rapidly transferred (< 5 s) into the SEM chamber to minimize air exposure.

Ultraviolet–Visible (UV–Vis) Spectroscopy. UV–vis data were collected using a Beckman Coulter DU 800 ultraviolet–visible (UV–vis) spectrophotometer. In an argon glovebox, the separator from the electrochemically tested Li–O₂ cells was removed and placed in a clean 20 mL vial. Next, 1.5 mL of DMSO-*d*₆ was added to the vial to dissolve the components in the separator. One milliliter of the solution was then placed in a sealed cuvette. The cuvette was removed from the glovebox, and UV–vis measurement was performed rapidly. The pristine solvent was used as a blank.

Nuclear Magnetic Resonance (NMR) Spectroscopy. NMR experiments were performed on a Bruker AVANCE or AVANCE III-400 MHz spectrometer. After the Li–O₂ cells were cycled, they were transferred into an argon glovebox without air exposure (MBRAUN, H₂O < 0.1 ppm, O₂ < 0.1 ppm). The cells were then placed in the glovebox antechamber (again without air exposure), and the cell was held under vacuum for about 10 min to remove some of the solvent. The separator and electrode were soaked in deuterated DMSO (DMSO-*d*₆ or DMSO-*d*₆ with TMS). The obtained NMR spectra were calibrated using the residual DMSO peak.

Quadrupole Time-of-Flight (Q-TOF) Mass Spectrometry.

After the electrochemical experiments were performed, the cells were moved to an argon glovebox without ambient exposure. The electrolyte-soaked separator was then removed from the cell and placed in a 5 mL vial. The vial was vacuumed in the glovebox antechamber to remove the DME solvent. Excess methanol was added, and Q-TOF analysis was performed on the supernatant. A Waters Q-TOF micro mass spectrometer equipped with an electrospray ionization ion source and a time-of-flight detector was used. The Q-TOF was run in ES+ mode meaning a proton is added to the neutral molecule before it enters the detector. Therefore, all of the reported *m/z* values for neutral molecules are a proton larger than the actual molecular weight of the molecule. The figures were calibrated with respect to the internal standard (quinine, *m/z* value of 325.19 and molecular weight of 324.42 g/mol).

RESULTS AND DISCUSSION

Influence on Discharge. The influence of TBA on the Li–O₂ discharge chemistry was studied by fabricating Li–O₂ cells with 0.1 M TBAClO₄ in 1,2-dimethoxyethane (DME) as the electrolyte. Figure 1a shows that TBAClO₄ in the electrolyte can support oxygen reduction at reaction voltages similar to those observed for Li–O₂ cells with LiClO₄ (~2.5 V_{Li}). Cyclic voltammetry has shown TBA is capable of complexing oxygen reduction products such as superoxide, and supporting the oxygen reduction and evolution process.^{7,9} However, TBA has not been incorporated and studied in conventional Li–O₂ cells. Although TBAClO₄ is the only salt introduced into the Li–O₂ cell, the discharge product obtained here appears to be Li₂O₂,

the desired discharge product in conventional Li–O₂ cells. Raman spectroscopy data in Figure 1b show peroxide vibration peaks at 250 and 790 cm⁻¹ that are typically associated with lithium peroxide.³⁷ We hypothesize that TBA complexes the superoxide intermediate (derived from oxygen reduction), bringing the superoxide intermediate into solution before allowing for coordination with lithium ions from the anode (Scheme 1). We do not expect to see TBA–superoxide as the final discharge product because lithium ions that originate from lithium metal oxidation during discharge would lead to disproportionation of the superoxide to peroxide (Scheme 1). X-ray diffraction (XRD) spectrum (Figure 1c) shows that the obtained Li₂O₂ discharge product is crystalline,³⁸ and the scanning electron microscope (SEM) image in Figure 1d reveals toroidal features typically associated with Li₂O₂, suggesting solution formation of Li₂O₂.³⁹ The effect of solvent on TBA-supported discharge was also explored, and in Figure S1, TBA can also support Li–O₂ discharge in DMSO and lead to Li₂O₂ formation. We cannot currently assign the XRD diffraction peaks at 43.6° and 50.5° 2θ range, but they appear to be a result of discharge as they are observed in DME and DMSO. These results in Figure 1a–d and Figure S1 indicate that a lithium salt added in the electrolyte is not required to support Li–O₂ discharge. Our finding was recently corroborated by Takechi et al.,⁴⁰ where they confirm Li₂O₂ formation in a lithium-salt free ionic liquid electrolyte. They show that an ammonium-based ionic liquid, similar to TBA, was capable of coordinating with superoxide, before Li⁺ released from a solid-state ionic conductor can displace the bulky cation to form Li₂O₂. In our work, the oxidation of lithium metal during discharge provides the lithium ions that are needed for Li₂O₂ formation. Any salt (e.g., TBAClO₄) capable of supporting oxygen reduction in combination with lithium metal can be utilized. Furthermore, the presence of TBAClO₄ does not appear to have a detrimental effect on the observed reaction voltage, at least on the first discharge.

Influence on Cycling. The effect of cation type (TBAClO₄ or LiClO₄) and solvent type (DME or DMSO) on cycling was also examined. Figure 2a shows the first and fifth cycles of three different electrolyte configurations in DME at a low current rate (3.95 μA/cm²). Current rates are based on geometric surface area of the carbon paper electrode. When 0.1 M LiClO₄ is used as the electrolyte, a discharge voltage at ~2.6 V is observed. However, complete charging requires voltages greater than 4 V, a behavior typically observed in the absence of catalysts¹⁸ or redox-mediator additives.²⁰ When 0.1 M TBAClO₄ is used as the electrolyte, the first discharge is similar to that obtained with 0.1 M LiClO₄, but a flat plateau at 3.55 V is observed almost during the entire charge. Furthermore, the charging profile for the 0.1 M TBA Li–O₂ cell remains similar at the fifth charge. When a mixture of TBAClO₄:LiClO₄ (2:1 molar ratio) is used as the electrolyte, charging behavior similar to a standard LiClO₄ cell is observed at the first charge. However, by the fifth cycle, charging occurs at 3.55 V (Figure 2a). The TBAClO₄:LiClO₄ Li–O₂ cell is certainly intermediate between the behavior observed for a LiClO₄-only cell and that for a TBAClO₄-only cell. The charging behavior in the presence of 0.1 M TBAClO₄ is reminiscent of redox mediator-like charging where iodide,¹⁹ TEMPO (2,2,6,6-tetramethylpiperidinyloxy),⁴¹ or TTF²⁰ can be oxidized during charge, and subsequent chemical reaction with Li₂O₂ leads to Li₂O₂ oxidation and reduction of the oxidized mediator. However, a redox-like mechanism does not seem likely for TBA because the nitrogen

functionality is already fully oxidized (+1). Some researchers have shown that when an ionic liquid such as Pyr₁₄TFSI (1-butyl-1-methylpyrrolidinium bis(trifluoromethanesulfonyl)imide) is used as part of the electrolyte, lower charging potentials are observed when compared to other organic electrolyte systems, despite the lack of catalysts or redox mediators.^{42–44} Those findings are similar to that observed here.

When the TBA concentration in the electrolyte is increased, the charging plateau is reduced, and the charging behavior at the fifth charge is improved when comparing 0.01 to 0.2 M TBA in DME (Figure 2b). However, there are limits to this surprising reduction in charging overpotentials in the presence of TBAClO₄. Figure 2c shows that as the current rate in DME is increased to 100 μA/cm², the ~3.55 V plateau is absent, and the charging curve resembles the LiClO₄-containing cells.

In DMSO, a different phenomenon is observed. At low current rates (3.95 μA/cm²), TBAClO₄ can support discharge and charge, but again the ~3.55 V plateau is absent (Figure S2) and it resembles the LiClO₄ cell. The plateau absence is also observed at 100 μA/cm²; however, the discharge capacities are higher when TBAClO₄ in DMSO is used as the electrolyte at high current rates. The improvement in discharge performance may be due to the ability of DMSO to stabilize superoxide species and solubilize TBA,²⁴ which is a superoxide complexing agent.¹⁰ At high current rates, there is a reduction in discharge capacity observed with cycling that may be due to the inability to completely oxidize the discharge products. In summary, the redox-like charging behavior induced by TBA appears rate- and solvent-dependent.

Effect on Li₂O₂ Oxidation. Although a stable 3.55 V charging plateau is observed when TBA is used as a salt in an ether solvent, it is important to know whether its presence can lead to Li₂O₂ oxidation. To study this, Li₂O₂-preloaded electrodes were fabricated. These electrodes consisted of Li₂O₂:Vulcan carbon:lithiated Nafion in a 1:1:1 mass ratio with no added catalysts. Other researchers have used these electrodes as a tool to study Li₂O₂ oxidation and eliminate the influence of other side reaction products that may have formed during cell discharge.^{18,45} Figure 3a shows current–time plots of these Li₂O₂-preloaded electrodes subjected to potentiostatic charging tests in different salt configurations in diglyme. Similar to work reported by Yao et al.,¹⁸ when 0.1 M LiClO₄ is used as the electrolyte, no oxidation current is observed at 3.9 V for 100 h. As expected, XRD spectra in Figure 3b show that Li₂O₂ is still present in the LiClO₄-containing electrode. However, when 0.1 M TBAClO₄ is used as the electrolyte at 3.7 or 3.9 V (above ~3.55 V), an oxidation current is observed. Remarkably, this corresponds to Li₂O₂ oxidation as Li₂O₂ is no longer observed on the electrode (Figure 3b). In addition, the Li₂O₂ is not converted to LiOH as LiOH is not observed on the electrode; no (101) or (110) diffraction peaks are found at 32.5° and 35.7° 2θ range.¹³ A Li₂O₂-preloaded cell is also held at open circuit with a 0.1 M TBAClO₄ electrolyte, and crystalline Li₂O₂ peaks are still observed. This further supports the notion that Li₂O₂ oxidation is not a result of chemical reaction with TBAClO₄, but the presence of an oxidizing voltage. Despite the lack of a stable oxidation plateau at around 3.55 V in DMSO (Figure S2), and the solvent-dependence of the charging profile, the presence of 0.1 M TBAClO₄ in DMSO also leads to the removal of Li₂O₂ during charge as the XRD spectrum in Figure S3 shows. Yao et al.¹⁸ showed that catalysts such as Ru and Cr are capable of oxidizing Li₂O₂ only when present in the

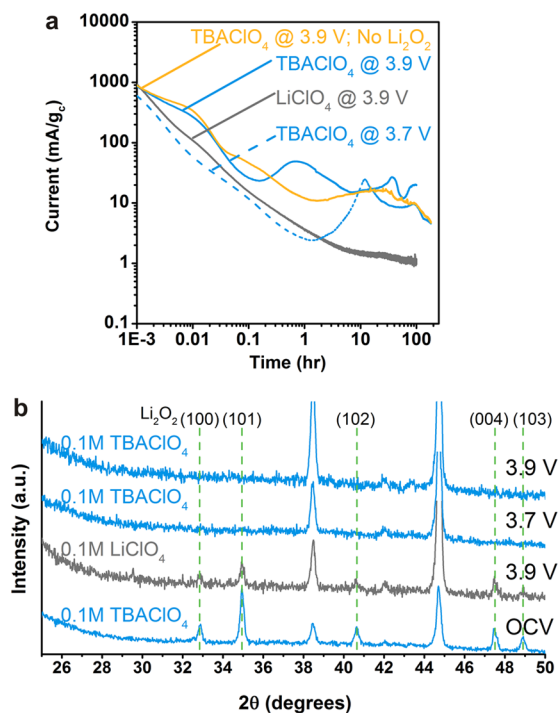


Figure 3. Li₂O₂ oxidation under potentiostatic hold. (a) Current versus time from potentiostatic holds at 3.7 or 3.9 V with or without Li₂O₂ preloaded in the electrode and with different salts in diglyme (0.1 M salt concentration). (b) Corresponding X-ray diffraction (XRD) spectra at the different voltages in (a). The “OCV” sample was held at open-circuit voltage for 200 h. Dashed lines in (b) are the (100), (101), (102), (004), and (103) Li₂O₂ diffraction peaks (left to right). Li–O₂ cell setup: Li metal/0.1 M LiClO₄ or TBAClO₄ salt in diglyme/Vulcan carbon + Nafion + Li₂O₂ (when present) on aluminum foil.

solid-state electrode, but not when the catalysts are in the electrolyte. Here, TBA appears to act as a redox mediator typically dissolved in the electrolyte (this hypothesis will be evaluated and discussed later).

The same charged Li₂O₂ electrodes examined by XRD in Figure 3 were studied using SEM. Figure 4 shows SEM images that further confirm the observations made in Figure 3, and show that the disappearance of the Li₂O₂ XRD peaks in Figure 3b is not due to a phase change between crystalline and amorphous Li₂O₂, but Li₂O₂ oxidation. The large solid particles seen in Figure 4a are the preloaded Li₂O₂, and they remain even after seating in a TBAClO₄ electrolyte at open-circuit voltage (OCV) for 200 h. In addition, Figure 4b shows that Li₂O₂ particles remain after the 3.9 V potentiostatic hold in 0.1 M LiClO₄, corroborating the XRD spectra in Figure 3b. When TBAClO₄ is used as the electrolyte, holes are observed where presumably Li₂O₂ particles used to be—further evidence of Li₂O₂ oxidation. Yao et al.⁴⁵ also used SEM to chronicle Li₂O₂ oxidation in the presence of perovskite and Cr nanoparticle-catalyzed Li₂O₂ electrodes, and attributed the disappearance of Li₂O₂ particles and appearance of these holes to be a result of Li₂O₂ oxidation. Because the 3.9 V 0.1 M TBAClO₄ cell was held for only 100 h, remnant partially oxidized Li₂O₂ particles can still be found (Figure S4), but their quantities are miniscule as compared to the OCV and LiClO₄-based cells. Furthermore, because the 3.7 V 0.1 M TBAClO₄-based preloaded cell was held for 200 h, no Li₂O₂ particles were found on the electrode after charging was completed.

Electrochemical Effect on TBA. TBA was examined in the absence of oxygen to decouple the mechanism of Li₂O₂ and TBA transformation. Figure 5a shows that because of the lack of oxygen, no significant discharge plateau is observed (as expected), but the ~3.55 V charging plateau is still present. However, the LiClO₄-based cells cycled in argon show no significant discharge or charge plateau (Figure S5). Furthermore, in Figure 3a, when the TBA electrolyte is held at 3.9 V with no Li₂O₂ present, there is a significant oxidation current. The cyclic voltammetry (CV) data in Figure 5b corroborate this observation as an oxidation current beginning at 3.5 V is observed when the TBAClO₄-containing electrolyte is scanned positively in argon. Again, no reduction current is observed in argon even after the TBA decomposition product is formed, indicating that TBA cannot act as a typical redox shuttle. The electrochemical-induced transformation of TBA appears irreversible, and reversibility is a requirement for any true redox shuttle. Therefore, in argon or O₂, TBA is electrochemically transformed during charge, and the TBA decomposition product leads to the oxidation of Li₂O₂ (when present). The mechanism that explains this behavior will be discussed in the next section.

Proposed Mechanism. ¹H NMR was used to determine the changes in the TBA chemical structure during cycling. The electrolyte-soaked separator from cycled Li–O₂ cells using 0.1 M TBAClO₄ or LiClO₄ in DME-based cells was extracted and soaked in deuterated DMSO for ¹H NMR and UV–vis analysis. In all TBA-based Li–O₂ cells in DME or diglyme where charging was performed, yellow coloration of the electrolyte was observed. UV–vis spectra in Figure S6 chronicle the presence of these light-absorbing species when cycling is performed using a TBA-based electrolyte, and additional species are formed when the cell is cycled in oxygen as compared to argon. Figure 6 shows ¹H NMR characterization of cells cycled with 0.1 M TBAClO₄ in argon and oxygen where new peaks related to TBA decomposition are observed. TBA is electrochemically transformed at 3.55 V (Figures 2 and 5) to form tributylamine (Figure 6) and possibly an alkene (Scheme 2). We propose an electrochemically induced formation of a base (from decomposition of carbon or electrolyte)^{46,47} at >3.5 V, which deprotonates TBA and allows TBA to undergo Hofmann elimination that leads to tributylamine and butene. The ¹H NMR peaks of commercial tributylamine match the newly observed TBA degradation peaks. Furthermore, quadrupole time-of-flight (Q-TOF) mass spectra in Figure 7 show a peak at an *m/z* value of 186.2 that corresponds to tributylamine (MW = 185.4 g/mol) and is formed after electrochemical-induced degradation in either argon or O₂. Finkelstein et al.⁴⁸ have previously shown that a quarternary ammonium salt can degrade to a tertiary amine and a hydrocarbon radical intermediate through a one-electron pathway. Assuming a one-electron decomposition pathway, Table S1 shows that complete decomposition of TBA should occur before seven charging steps, and Figure S7 shows evidence that the charging voltage begins to increase at the seventh charge. However, NMR data in Figure 6 show TBA is still present after 15 cycles in O₂. Therefore, it is possible that during charging, TBA decomposition products can also be electrochemically oxidized as well as some direct delithiation of Li₂O₂ that can occur below 4 V.⁴⁹

The proposed TBA reaction pathway is shown in Scheme 2. The alkene formed here would be butene, but the low boiling point of butene (−6.5 °C) makes postcycling characterization

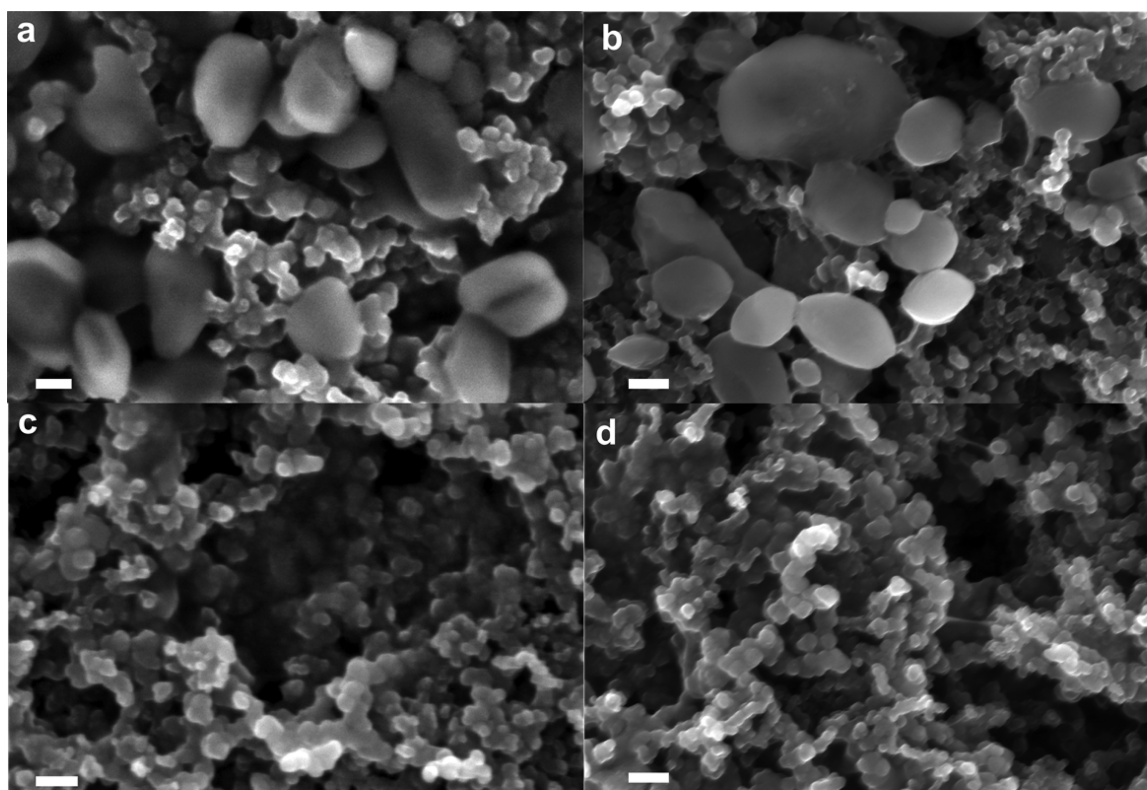


Figure 4. SEM micrographs chronicling the electrochemical changes in Figure 3. (a) Li_2O_2 -preloaded electrode held at open-circuit voltage (OCV) in 0.1 M TBAClO_4 for 200 h, (b) at 3.9 V in 0.1 M LiClO_4 for 100 h, (c) at 3.7 V in 0.1 M TBAClO_4 for 200 h, and (d) at 3.9 V in 0.1 M TBAClO_4 for 100 h. Solvent = diglyme. Li– O_2 cell setup: Li metal/0.1 M LiClO_4 or TBAClO_4 salt in diglyme/Vulcan carbon + Nafion + Li_2O_2 on aluminum foil (scale bar = 200 nm).

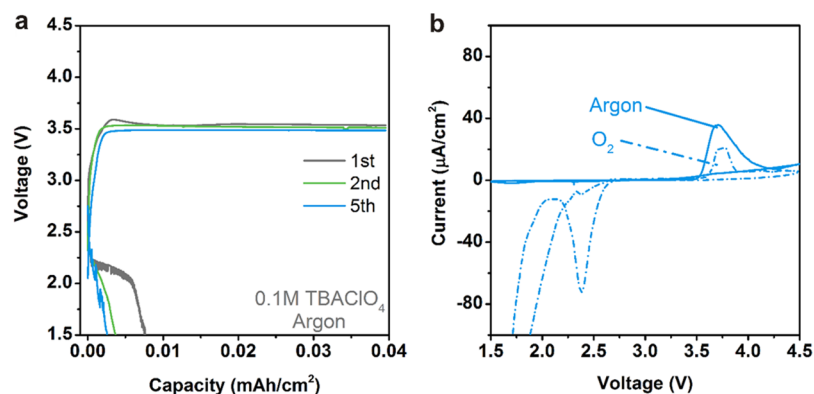


Figure 5. Electrochemical-induced transformation of TBA. (a) Cycling using 0.1 M TBAClO_4 in DME at $3.95 \mu\text{A}/\text{cm}^2$ to $0.04 \text{mAh}/\text{cm}^2$ in argon. (b) Cyclic voltammetry (two-electrode setup) in argon and O_2 at 0.1 mV/s scan rate with a 0.1 M TBAClO_4 in DME electrolyte. Li– O_2 cell setup for (a): Li metal/0.1 M TBAClO_4 in DME/carbon paper. Setup for (b): working electrode, carbon paper; reference and counter electrode, lithium metal. CV was performed by scanning first to 4.5 V before scanning to 1.5 V. The second cycle for both argon and O_2 is shown in (b).

difficult. OCV experiments in Figure 3b and chemical experiments involving a 10:10:1 molar ratio of Li_2O_2 : KO_2 : TBAClO_4 in Figure S8 show that TBA does not appear to chemically react with Li_2O_2 to oxidize Li_2O_2 . Once tributylamine and butene are formed, they can possibly undergo reactions with Li_2O_2 . To examine this, a Li_2O_2 -preloaded electrode is held at OCV in commercial tributylamine or decene (chemically similar to butene but is a liquid at room temperature) for 200 h, and XRD is performed after (Figure S9). XRD shows that Li_2O_2 is still present; hence, the oxidation of Li_2O_2 is not due to chemical reaction between Li_2O_2 and tributylamine or butene alone. A stirred chemical

mixture of Li_2O_2 with tributylamine or decene also does not reveal any changes in the ^1H NMR spectra (Figures S10 and S11), further confirming the XRD observation in Figure S9. The lack of bulk reaction between tributylamine and Li_2O_2 is surprising because it is known that tertiary amines can react with H_2O_2 to form amine oxides;^{50,51} however, Hoh et al.⁵¹ noted that direct oxidation of tertiary amines with H_2O_2 proceeds slowly. The limited solubility of Li_2O_2 in tributylamine would also diminish an already slow reaction with tributylamine as compared to H_2O_2 . Other researchers have shown that oxygen can react with tertiary amines to form an amine oxide, and the amine oxide is an intermediate that is

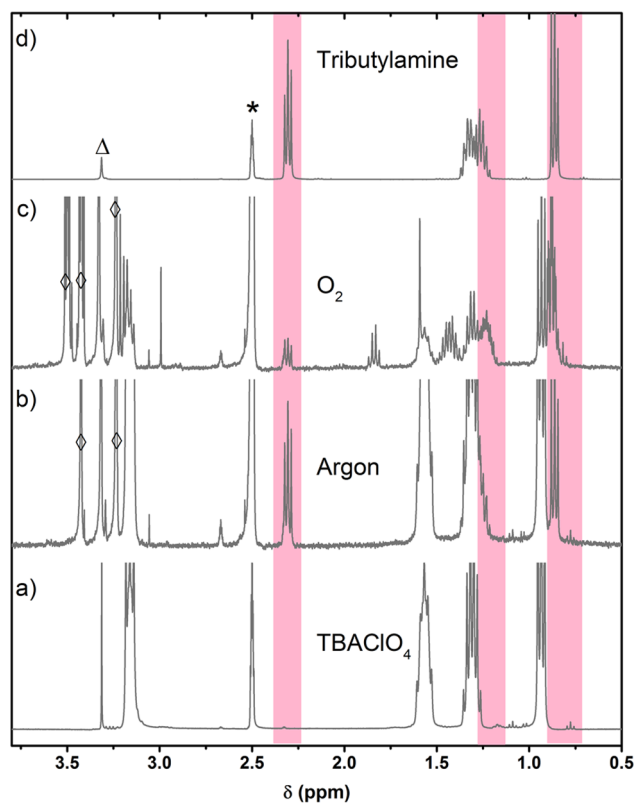


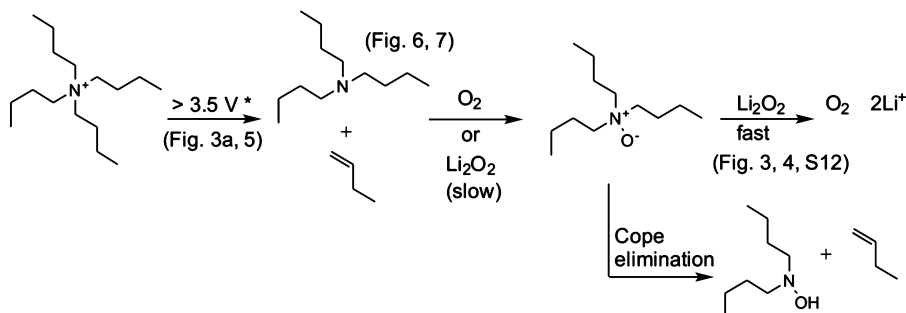
Figure 6. ¹H NMR after Li–O₂ cycling in argon and oxygen. ¹H NMR (400 MHz; DMSO-*d*₆; H-DMSO) spectrum of (a) TBAClO₄, (b) electrolyte of Li–O₂ cell after five cycles in argon, (c) electrolyte of Li–O₂ cell after 15 cycles in oxygen, and (d) commercial tributylamine. * = DMSO, Δ = H₂O, ◇ = solvent. Spectra were calibrated using the residual DMSO (“H-DMSO”) peak in DMSO-*d*₆. Integration values for peaks in (b) and (c) are in Table S2. Li–O₂ cell setup: Li metal/0.1 M TBAClO₄ in DME/carbon paper. The actual cycling profile for (b) is shown in Figure 2a, and for (c) it is shown in Figure S7.

difficult to characterize because it undergoes subsequent reactions.^{52,53} Some of these possible reactions are shown in Scheme 2. One reaction the tributylamine oxide can undergo is Cope elimination,^{52,54} an intra- or intermolecular reaction that involves the oxygen on the tertiary amine oxide abstracting a hydrogen from a carbon that is β to the nitrogen to form an

olefin. In addition, alkyl radicals and nitroxide can also be formed.⁵²

Therefore, we hypothesize that tributylamine can react with oxygen (or Li₂O₂) to form a tributylamine oxide intermediate. The amine oxide, when formed, can react with Li₂O₂ to release Li⁺ and O₂. This reaction between the amine oxide intermediate and Li₂O₂ is responsible for the Li₂O₂ oxidation observed after charging in the XRD and SEM data (Figures 3 and 4). It is also possible that the generated nitroxide (from alkyl radical loss) can react with Li₂O₂ to oxidize it as a similar nitroxide, TEMPO, has been shown to oxidize Li₂O₂ during charging.⁴¹ The mechanism shown in Scheme 2 explains our observations, but cannot encompass all of the possible decomposition products formed as tertiary amine oxides are known to structurally rearrange to yield other products.⁵² The extra ¹H NMR peaks observed in O₂ (not including the tributylamine peaks) could be due to decomposition products that result from the amine oxide reaction with Li₂O₂, Cope elimination, etc. In argon (Figure 6b), only tributylamine is present, because the lack of O₂ or Li₂O₂ in the argon cells precludes the formation of tributylamine oxide and the presence of additional peaks. To test this hypothesis, we mix trimethylamine oxide (as proxy for tributylamine oxide) with Li₂O₂ in acetonitrile, and the characteristic yellow color was observed, a color observed electrochemically (after cycling) in our experiments and by Hoh et al.⁵¹ in the mixture of tertiary amine with H₂O₂ at higher temperatures. New peaks also arise in the NMR spectra (Figure S12). Therefore, next-generation Li–O₂ cells can be fabricated to include amine oxides as a tool to reduce Li₂O₂ charging voltages. Unfortunately, the amine oxide, once formed, cannot revert to the original TBA to make this system an ideal redox mediator. We noted earlier that lower charging overpotentials were observed for Pyr₁₄TFSI-based Li–O₂ cells despite the lack of catalysts or redox mediators.^{42–44} However, no clear mechanistic explanation was provided in those papers to explain the low overpotentials. Other researchers have shown that Pyr₁₄TFSI, like TBA, can undergo Hofmann elimination.^{55,56} Therefore, the low charging potentials observed in those works are due to a similar mechanism observed in this work. At the low potential, instead of bulk Li₂O₂ oxidation, pyrrolidinium undergoes Hofmann elimination to form a tertiary amine and alkene.⁵⁵ The amine formed can then react with O₂ to form an amine oxide and lead to the decomposition of Li₂O₂.

Scheme 2. Mechanism for TBA-Supported Li₂O₂ Oxidation^a



^aProposed mechanism of electrochemical-induced transformation of tetrabutylammonium to form tributylamine, and the subsequent oxidation of Li₂O₂ to release oxygen. The figure numbers in parentheses in the mechanism indicate the figure in this Article that provides evidence of the stated pathway. ClO₄[−] anion is omitted in the mechanism scheme for clarity. Li–O₂ cell setup: Li metal/0.1 M TBAClO₄ in DME/carbon paper. *At > 3.5 V, electrochemical-induced base formation deprotonates TBA, allowing TBA to undergo Hofmann elimination.

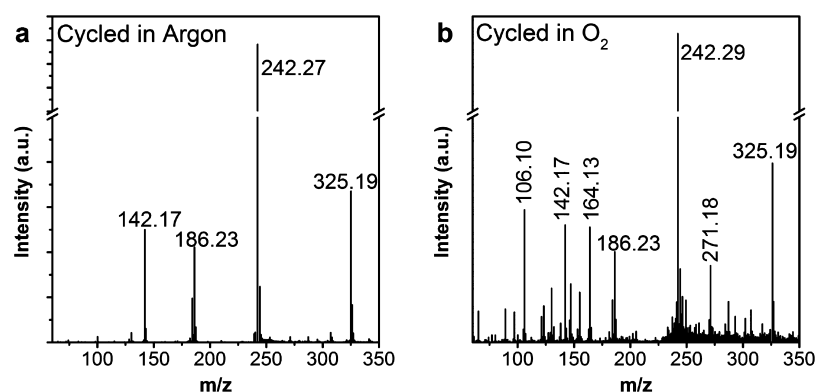


Figure 7. Quadrupole time-of-flight (Q-TOF) mass spectra after Li–O₂ cycling. Spectra obtained after cycling in (a) argon and (b) oxygen. Li–O₂ cell setup: Li metal|0.1 M TBAClO₄ in DME|carbon paper. For neutral molecules, a proton is added to the molecule by the electron source before detection; therefore, MW = m/z value – 1 for neutral molecules. Known assignments: internal standard (quinine, neutral, m/z = 325.19, MW = 324.42 g/mol), tetrabutylammonium (charged, m/z = 242.3, MW = 242.5 g/mol), and tributylamine (neutral, m/z = 186.2, MW = 185.4 g/mol). Additional structures that may correspond to the unassigned m/z value shown in this figure are listed in Figure S13. MW = molecular weight.

The electrochemical-induced decomposition of TBA is irreversible, and as Mousavi et al.⁵⁷ recently reported, changing the chain length, size, and type of branching on the ammonium cation may not improve the electrochemical stability.

CONCLUSIONS

We have shown that Li–O₂ discharge and charge can occur in the absence of lithium-based salts. Ammonium-based electrolytes in the presence of lithium metal can support the formation of Li₂O₂ during discharge, where TBA can temporarily complex superoxide in solution before Li ions from the oxidized lithium metal anode combine to form Li₂O₂. During charge, TBA-based electrolytes can lead to charging voltages below 4 V at low current rates, leading to a 0.5 V improvement over LiClO₄-based electrolytes. TBA concentration and solvent type (ether vs DMSO) were also studied and were shown to influence the observed discharge and charge performance. Furthermore, we proposed a mechanism to explain the ability of TBA to support Li₂O₂ oxidation. Electrochemically induced degradation of TBA occurs at 3.55 V to form a tertiary amine that can react with oxygen (or Li₂O₂) to form an amine oxide; the amine oxide reacts with Li₂O₂ in a faster reaction to release O₂ and Li⁺. Unfortunately, TBA decomposition is irreversible. The decomposition mechanism developed here can also help explain the unusually low charging overpotentials observed when ionic liquids like Pyr₁₄TFSI are used in a Li–O₂ cell. We have shown TBA can support discharge and charge in Li–O₂ cells, and amine oxides can oxidize Li₂O₂ in Li–O₂ cells. Knowledge gained from this work should allow for the development of newer salts, and broaden our understanding of Li₂O₂ oxidation mechanisms.

ASSOCIATED CONTENT

Supporting Information

The Supporting Information is available free of charge on the ACS Publications website at DOI: 10.1021/acs.jpcc.7b05322.

Additional calculations, electrochemical data, and XRD, SEM, UV–vis, and NMR data (PDF)

AUTHOR INFORMATION

Corresponding Author

*E-mail: hammond@mit.edu.

ORCID

Paula T. Hammond: 0000-0002-9835-192X

Notes

The authors declare no competing financial interest.

ACKNOWLEDGMENTS

This work was supported in part by the Samsung Advanced Institute of Technology (SAIT), and the facilities at the Koch Institute for Integrative Cancer Research. C.V.A. is supported by the U.S. Department of Defense (DoD) through the National Defense Science and Engineering Graduate (NDSEG) Fellowship, and the Alfred P. Sloan Foundation's Minority Ph.D. Program. This work made use of the Shared Experimental Facilities supported by the MRSEC Program of the National Science Foundation under award number DMR-1419807. We also thank Professor Yang Shao-Horn for providing access to her laboratory and equipment, and Li Li for performing the Q-TOF experiment and for helpful discussions.

REFERENCES

- (1) Bruce, P. G.; Freunberger, S. A.; Hardwick, L. J.; Tarascon, J.-M. Li–O₂ and Li–S Batteries with High Energy Storage. *Nat. Mater.* **2011**, *11*, 19–29.
- (2) Scrosati, B.; Hassoun, J.; Sun, Y.-K. Lithium-Ion Batteries. A Look into the Future. *Energy Environ. Sci.* **2011**, *4*, 3287–3295.
- (3) Girishkumar, G.; McCloskey, B.; Luntz, A.; Swanson, S.; Wilcke, W. Lithium–Air Battery: Promise and Challenges. *J. Phys. Chem. Lett.* **2010**, *1*, 2193–2203.
- (4) Kwabi, D.; Ortiz-Vitoriano, N.; Freunberger, S.; Chen, Y.; Imanishi, N.; Bruce, P.; Shao-Horn, Y. Materials Challenges in Rechargeable Lithium–Air Batteries. *MRS Bull.* **2014**, *39*, 443–452.
- (5) Lu, Y.-C.; Gallant, B. M.; Kwabi, D. G.; Harding, J. R.; Mitchell, R. R.; Whittingham, M. S.; Shao-Horn, Y. Lithium–Oxygen Batteries: Bridging Mechanistic Understanding and Battery Performance. *Energy Environ. Sci.* **2013**, *6*, 750–768.
- (6) Peng, Z.; Freunberger, S. A.; Chen, Y.; Bruce, P. G. A Reversible and Higher-Rate Li–O₂ Battery. *Science* **2012**, *337*, 563–566.
- (7) Laoire, C. O.; Mukerjee, S.; Abraham, K.; Plichta, E. J.; Hendrickson, M. A. Elucidating the Mechanism of Oxygen Reduction for Lithium–Air Battery Applications. *J. Phys. Chem. C* **2009**, *113*, 20127–20134.
- (8) Amanchukwu, C. V.; Chang, H.-H.; Gauthier, M.; Feng, S.; Batcho, T. P.; Hammond, P. T. One-Electron Mechanism in a Gel–

Polymer Electrolyte Li–O₂ Battery. *Chem. Mater.* **2016**, *28*, 7167–7177.

(9) Laoire, C. O.; Mukerjee, S.; Abraham, K.; Plichta, E. J.; Hendrickson, M. A. Influence of Nonaqueous Solvents on the Electrochemistry of Oxygen in the Rechargeable Lithium–Air Battery. *J. Phys. Chem. C* **2010**, *114*, 9178–9186.

(10) Kwabi, D. G.; Bryantsev, V. S.; Batcho, T. P.; Itkis, D. M.; Thompson, C. V.; Shao-Horn, Y. Experimental and Computational Analysis of the Solvent-Dependent O₂/Li⁺-O₂⁻ Redox Couple: Standard Potentials, Coupling Strength, and Implications for Lithium–Oxygen Batteries. *Angew. Chem.* **2016**, *128*, 3181–3186.

(11) Black, R.; Oh, S. H.; Lee, J.-H.; Yim, T.; Adams, B.; Nazar, L. F. Screening for Superoxide Reactivity in Li–O₂ Batteries: Effect on Li₂O₂/LiOH Crystallization. *J. Am. Chem. Soc.* **2012**, *134*, 2902–2905.

(12) Radin, M. D.; Siegel, D. J. Charge Transport in Lithium Peroxide: Relevance for Rechargeable Metal–Air Batteries. *Energy Environ. Sci.* **2013**, *6*, 2370–2379.

(13) Kwabi, D. G.; Batcho, T. P.; Amanchukwu, C. V.; Ortiz-Vitoriano, N.; Hammond, P.; Thompson, C. V.; Shao-Horn, Y. Chemical Instability of Dimethyl Sulfoxide in Lithium–Air Batteries. *J. Phys. Chem. Lett.* **2014**, *5*, 2850–2856.

(14) Younesi, R.; Hahlin, M.; Treskow, M.; Scheers, J.; Johansson, P.; Edström, K. Ether Based Electrolyte, LiB(CN)₄ Salt and Binder Degradation in the Li–O₂ Battery Studied by Hard X-Ray Photoelectron Spectroscopy (HAXPES). *J. Phys. Chem. C* **2012**, *116*, 18597–18604.

(15) Amanchukwu, C. V.; Gauthier, M.; Batcho, T. P.; Symister, C.; Shao-Horn, Y.; D'Arcy, J. M.; Hammond, P. T. Evaluation and Stability of Pedot Polymer Electrodes for Li–O₂ Batteries. *J. Phys. Chem. Lett.* **2016**, *7*, 3770–3775.

(16) McCloskey, B.; Speidel, A.; Scheffler, R.; Miller, D.; Viswanathan, V.; Hummelshøj, J.; Nørskov, J.; Luntz, A. Twin Problems of Interfacial Carbonate Formation in Nonaqueous Li–O₂ Batteries. *J. Phys. Chem. Lett.* **2012**, *3*, 997–1001.

(17) Amanchukwu, C. V.; Harding, J. R.; Shao-Horn, Y.; Hammond, P. T. Understanding the Chemical Stability of Polymers for Lithium–Air Batteries. *Chem. Mater.* **2015**, *27*, 550–561.

(18) Yao, K. P.; Risch, M.; Sayed, S. Y.; Lee, Y.-L.; Harding, J. R.; Grimaud, A.; Pour, N.; Xu, Z.; Zhou, J.; Mansour, A. Solid-State Activation of Li₂O₂ Oxidation Kinetics and Implications for Li–O₂ Batteries. *Energy Environ. Sci.* **2015**, *8*, 2417–2426.

(19) Lim, H. D.; Song, H.; Kim, J.; Gwon, H.; Bae, Y.; Park, K. Y.; Hong, J.; Kim, H.; Kim, T.; Kim, Y. H. Superior Rechargeability and Efficiency of Lithium–Oxygen Batteries: Hierarchical Air Electrode Architecture Combined with a Soluble Catalyst. *Angew. Chem., Int. Ed.* **2014**, *53*, 3926–3931.

(20) Chen, Y.; Freunberger, S. A.; Peng, Z.; Fontaine, O.; Bruce, P. G. Charging a Li–O₂ Battery Using a Redox Mediator. *Nat. Chem.* **2013**, *5*, 489–494.

(21) Yoshida, K.; Nakamura, M.; Kazue, Y.; Tachikawa, N.; Tsuzuki, S.; Seki, S.; Dokko, K.; Watanabe, M. Oxidative-Stability Enhancement and Charge Transport Mechanism in Glyme–Lithium Salt Equimolar Complexes. *J. Am. Chem. Soc.* **2011**, *133*, 13121–13129.

(22) Aetukuri, N. B.; McCloskey, B. D.; García, J. M.; Krupp, L. E.; Viswanathan, V.; Luntz, A. C. Solvating Additives Drive Solution-Mediated Electrochemistry and Enhance Toroid Growth in Nonaqueous Li–O₂ Batteries. *Nat. Chem.* **2015**, *7*, 50–56.

(23) Burke, C. M.; Pande, V.; Khetan, A.; Viswanathan, V.; McCloskey, B. D. Enhancing Electrochemical Intermediate Solvation through Electrolyte Anion Selection to Increase Nonaqueous Li–O₂ Battery Capacity. *Proc. Natl. Acad. Sci. U. S. A.* **2015**, *112*, 9293–9298.

(24) Johnson, L.; Li, C.; Liu, Z.; Chen, Y.; Freunberger, S. A.; Ashok, P. C.; Praveen, B. B.; Dholakia, K.; Tarascon, J.-M.; Bruce, P. G. The Role of LiO₂ Solubility in O₂ Reduction in Aprotic Solvents and Its Consequences for Li–O₂ Batteries. *Nat. Chem.* **2014**, *6*, 1091–1099.

(25) Gao, X.; Chen, Y.; Johnson, L.; Bruce, P. G. Promoting Solution Phase Discharge in Li–O₂ Batteries Containing Weakly Solvating Electrolyte Solutions. *Nat. Mater.* **2016**, *15*, 882–888.

(26) Khetan, A.; Luntz, A.; Viswanathan, V. Trade-Offs in Capacity and Rechargeability in Nonaqueous Li–O₂ Batteries: Solution-Driven Growth Versus Nucleophilic Stability. *J. Phys. Chem. Lett.* **2015**, *6*, 1254–1259.

(27) Schmeisser, M.; Illner, P.; Puchta, R.; Zahl, A.; van Eldik, R. Gutmann Donor and Acceptor Numbers for Ionic Liquids. *Chem. - Eur. J.* **2012**, *18*, 10969–10982.

(28) Jozwiuk, A.; Berkes, B. B.; Weiß, T.; Sommer, H.; Janek, J.; Brezesinski, T. The Critical Role of Lithium Nitrate in the Gas Evolution of Lithium–Sulfur Batteries. *Energy Environ. Sci.* **2016**, *9*, 2603–2608.

(29) Walker, W.; Giordani, V.; Uddin, J.; Bryantsev, V. S.; Chase, G. V.; Addison, D. A Rechargeable Li–O₂ Battery Using a Lithium Nitrate/N, N-Dimethylacetamide Electrolyte. *J. Am. Chem. Soc.* **2013**, *135*, 2076–2079.

(30) Schwenke, K. U.; Metzger, M.; Restle, T.; Piana, M.; Gasteiger, H. A. The Influence of Water and Protons on Li₂O₂ Crystal Growth in Aprotic Li–O₂ Cells. *J. Electrochem. Soc.* **2015**, *162*, A573–A584.

(31) Frith, J. T.; Russell, A. E.; Garcia-Araez, N.; Owen, J. R. An In-Situ Raman Study of the Oxygen Reduction Reaction in Ionic Liquids. *Electrochem. Commun.* **2014**, *46*, 33–35.

(32) Dietzel, P. D.; Kremer, R. K.; Jansen, M. Tetraorganylammonium Superoxide Compounds: Close to Unperturbed Superoxide Ions in the Solid State. *J. Am. Chem. Soc.* **2004**, *126*, 4689–4696.

(33) Allen, C. J.; Hwang, J.; Kautz, R.; Mukerjee, S.; Plichta, E. J.; Hendrickson, M. A.; Abraham, K. Oxygen Reduction Reactions in Ionic Liquids and the Formulation of a General ORR Mechanism for Li–Air Batteries. *J. Phys. Chem. C* **2012**, *116*, 20755–20764.

(34) Peng, Z.; Freunberger, S. A.; Hardwick, L. J.; Chen, Y.; Giordani, V.; Bardé, F.; Novák, P.; Graham, D.; Tarascon, J. M.; Bruce, P. G. Oxygen Reactions in a Non-Aqueous Li⁺ Electrolyte. *Angew. Chem.* **2011**, *123*, 6475–6479.

(35) Yang, L.; Frith, J.; Garcia-Araez, N.; Owen, J. R. A New Method to Prevent Degradation of Lithium–Oxygen Batteries: Reduction of Superoxide by Viologen. *Chem. Commun.* **2015**, *51*, 1705–1708.

(36) Gallant, B. M.; Mitchell, R. R.; Kwabi, D. G.; Zhou, J.; Zuin, L.; Thompson, C. V.; Shao-Horn, Y. Chemical and Morphological Changes of Li–O₂ Battery Electrodes Upon Cycling. *J. Phys. Chem. C* **2012**, *116*, 20800–20805.

(37) Gittleson, F. S.; Yao, K. P.; Kwabi, D. G.; Sayed, S. Y.; Ryu, W. H.; Shao-Horn, Y.; Taylor, A. D. Raman Spectroscopy in Lithium–Oxygen Battery Systems. *ChemElectroChem* **2015**, *2*, 1446–1457.

(38) Lu, Y.-C.; Kwabi, D. G.; Yao, K. P.; Harding, J. R.; Zhou, J.; Zuin, L.; Shao-Horn, Y. The Discharge Rate Capability of Rechargeable Li–O₂ Batteries. *Energy Environ. Sci.* **2011**, *4*, 2999–3007.

(39) Mitchell, R. R.; Gallant, B. M.; Thompson, C. V.; Shao-Horn, Y. All-Carbon-Nanofiber Electrodes for High-Energy Rechargeable Li–O₂ Batteries. *Energy Environ. Sci.* **2011**, *4*, 2952–2958.

(40) Takechi, K.; Singh, N.; Arthur, T. S.; Mizuno, F. Decoupling Energy Storage from Electrochemical Reactions in Li–Air Batteries toward Achieving Continuous Discharge. *ACS Energy Letters* **2017**, *2*, 694–699.

(41) Bergner, B. J.; Schürmann, A.; Pepler, K.; Garsuch, A.; Janek, J. r. Tempo: A Mobile Catalyst for Rechargeable Li–O₂ Batteries. *J. Am. Chem. Soc.* **2014**, *136*, 15054–15064.

(42) Elia, G.; Hassoun, J.; Kwak, W.-J.; Sun, Y.-K.; Scrosati, B.; Mueller, F.; Bresser, D.; Passerini, S.; Oberhumer, P.; Tsiouvaras, N. An Advanced Lithium–Air Battery Exploiting an Ionic Liquid-Based Electrolyte. *Nano Lett.* **2014**, *14*, 6572–6577.

(43) Xie, J.; Dong, Q.; Madden, I.; Yao, X.; Cheng, Q.; Dornath, P.; Fan, W.; Wang, D. Achieving Low Overpotential Li–O₂ Battery Operations by Li₂O₂ Decomposition through One-Electron Processes. *Nano Lett.* **2015**, *15*, 8371–8376.

(44) Elia, G. A.; Bresser, D.; Reiter, J.; Oberhumer, P.; Sun, Y.-K.; Scrosati, B.; Passerini, S.; Hassoun, J. Interphase Evolution of a Lithium-Ion/Oxygen Battery. *ACS Appl. Mater. Interfaces* **2015**, *7*, 22638–22643.

(45) Yao, K. P.; Lu, Y.-C.; Amanchukwu, C. V.; Kwabi, D. G.; Risch, M.; Zhou, J.; Grimaud, A.; Hammond, P. T.; Bardé, F.; Shao-Horn, Y. The Influence of Transition Metal Oxides on the Kinetics of Li_2O_2 Oxidation in $\text{Li}-\text{O}_2$ Batteries: High Activity of Chromium Oxides. *Phys. Chem. Chem. Phys.* **2014**, *16*, 2297–2304.

(46) Ottakam Thotiyl, M. M.; Freunberger, S. A.; Peng, Z.; Bruce, P. G. The Carbon Electrode in Nonaqueous $\text{Li}-\text{O}_2$ Cells. *J. Am. Chem. Soc.* **2012**, *135*, 494–500.

(47) McCloskey, B.; Bethune, D.; Shelby, R.; Girishkumar, G.; Luntz, A. Solvents' Critical Role in Nonaqueous Lithium–Oxygen Battery Electrochemistry. *J. Phys. Chem. Lett.* **2011**, *2*, 1161–1166.

(48) Finkelstein, M.; Petersen, R. C.; Ross, S. D. The Electrochemical Degradation of Quaternary Ammonium Salts. *J. Am. Chem. Soc.* **1959**, *81*, 2361–2364.

(49) Lu, Y.-C.; Shao-Horn, Y. Probing the Reaction Kinetics of the Charge Reactions of Nonaqueous $\text{Li}-\text{O}_2$ Batteries. *J. Phys. Chem. Lett.* **2012**, *4*, 93–99.

(50) Cope, A. C.; LeBel, N. A.; Lee, H.-H.; Moore, W. R. Amine Oxides. iii. Selective Formation of Olefins from Unsymmetrical Amine Oxides and Quaternary Ammonium Hydroxides. *J. Am. Chem. Soc.* **1957**, *79*, 4720–4729.

(51) Hoh, G.; Barlow, D.; Chadwick, A.; Lake, D.; Sheeran, S. Hydrogen Peroxide Oxidation of Tertiary Amines. *J. Am. Oil Chem. Soc.* **1963**, *40*, 268–271.

(52) Slagle, I. R.; Dudich, J. F.; Gutman, D. Identification of Reactive Routes in the Reactions of Oxygen Atoms with Methylamine, Dimethylamine, Trimethylamine, Ethylamine, Diethylamine, and Triethylamine. *J. Phys. Chem.* **1979**, *83*, 3065–3070.

(53) Cullis, C.; Waddington, D. *Proc. R. Soc. A*; The Royal Society: UK, 1958; Vol. 246, pp 91–98.

(54) Cope, A. C.; Foster, T. T.; Towle, P. H. Thermal Decomposition of Amine Oxides to Olefins and Dialkylhydroxylamines. *J. Am. Chem. Soc.* **1949**, *71*, 3929–3934.

(55) Schwenke, K. U.; Herranz, J.; Gasteiger, H. A.; Piana, M. Reactivity of the Ionic Liquid $\text{Py}_{14}\text{TFSI}$ with Superoxide Radicals Generated from KO_2 or by Contact of O_2 with $\text{Li}_7\text{Ti}_5\text{O}_{12}$. *J. Electrochem. Soc.* **2015**, *162*, A905–A914.

(56) Long, H.; Kim, K.; Pivovar, B. S. Hydroxide Degradation Pathways for Substituted Trimethylammonium Cations: A DFT Study. *J. Phys. Chem. C* **2012**, *116*, 9419–9426.

(57) Mousavi, M. P.; Kashfolgheta, S.; Stein, A.; Bühlmann, P. Electrochemical Stability of Quaternary Ammonium Cations: An Experimental and Computational Study. *J. Electrochem. Soc.* **2016**, *163*, H74–H80.